Article

Snowpack Aging, Water Isotope Evolution, and Runoff Isotope Signals, Palouse Range, Idaho, USA

Jeff B. Langman [1,*] , Julianna Martin [1], Ethan Gaddy [1], Jan Boll [2] and David Behrens [1]

1   Department of Earth and Spatial Sciences, University of Idaho, Moscow, ID 83844, USA;
     mart8224@vandals.uidaho.edu (J.M.); gadd5510@vandals.uidaho.edu (E.G.);
     behr2699@vandals.uidaho.edu (D.B.)
2   Department of Civil and Environmental Engineering, Washington State University, Pullman, WA 99164, USA;
     j.boll@wsu.edu
*   Correspondence: jlangman@uidaho.edu; Tel.: +1-208-885-0310

Abstract: A snowpack's δ^2H and δ^{18}O values evolve with snowfall, sublimation, evaporation, and melt, which produces temporally variable snowpack, snowmelt, and runoff isotope signals. As a snowpack ages, the relatively depleted δ^2H and δ^{18}O values of snow will become less depleted with sublimation and evaporation, and the internal distribution of isotope signals is altered with melt moving through and out of the snowpack. An examination of δ^2H and δ^{18}O values for snowpack, snowmelt, and ephemeral creek water in the Palouse Range of northern Idaho indicated an evolution from variably depleted snowpack to enriched snowmelt and relatively consistent isotope signals in springtime ephemeral creeks. Within the primary snow band of the mountain range and during the winter–spring period of 2019–2020, the snowpack had an isotope range of -130 to -75‰ for δ^2H and -18 to -10.5‰ for δ^{18}O with resulting snowmelt values of -120 to -90‰ for δ^2H and -16.5 to -12.5‰ for δ^{18}O. With runoff of snowmelt to ephemeral creeks, the isotope values compressed to -107 to -104‰ for δ^2H and -15.5 to -14.5‰ for δ^{18}O. Aging of the snowpack produced increasing densities in the base, middle, and upper layers along with a corresponding enrichment of isotope values. The highest elevation site indicated the least enrichment of δ^2H and δ^{18}O in the snowpack base layer, and the lowest elevation site indicated the strongest enrichment of δ^2H and δ^{18}O in the snowpack base layer. Deuterium excess decreased with snowpack aging processes of accumulation and melt release, along with the migration of water vapor and snowmelt within the snowpack. It is likely that winter melt (early depleted signal) is a primary contributor to creeks and groundwater along the Palouse Range, but the strong variability of snowpack isotope signals provides a wide range of possible isotope signals to surface-water and groundwater systems at the mountain front.

Keywords: water isotopes; snowpack aging; snowmelt isotope evolution

1. Introduction

Snow is an important hydrologic reservoir that has been exploited as a natural cycle of seasonally available water [1–6]. The stable isotopes of water (δ^2H and δ^{18}O) can be used to identify source waters and flowpaths [7–14], but the tracing of snow/snowmelt through a surface- and/or groundwater system can be difficult due to the temporal effect on isotope values with sublimation/evaporation during accumulation (snowpack), melt, and runoff/infiltration [15–22]. These temporal influences can result in dynamic water stores that contribute potential source waters with variable isotopic signals throughout the seasonal cycle of snowfall → snowpack → snowmelt [16,23–26]. However, a snowpack typically contains fewer heavy isotopes (^{2}H and ^{18}O) compared to non-winter precipitation, which can allow for the tracing of snowmelt to other hydrologic systems [16,27–30]. The goal of this study was to evaluate the seasonal evolution, or trend, of snowpack isotope signals at multiple elevations and depths, and in turn, understand snowmelt and runoff

isotope signals in the snow-dominated Palouse Range of northern Idaho, USA (Figure 1). It was expected that the isotopic lapse rate would produce different isotope signals in the snowpack by elevation [16,25,27] and snowpack evolution, or snowpack aging, would produce seasonal trends in δ^2H, δ^{18}O, and deuterium excess (d-excess). This study was part of a larger study examining water isotope signals within the South Fork Palouse River Basin and connections between source waters and surface-water and groundwater systems [31–34].
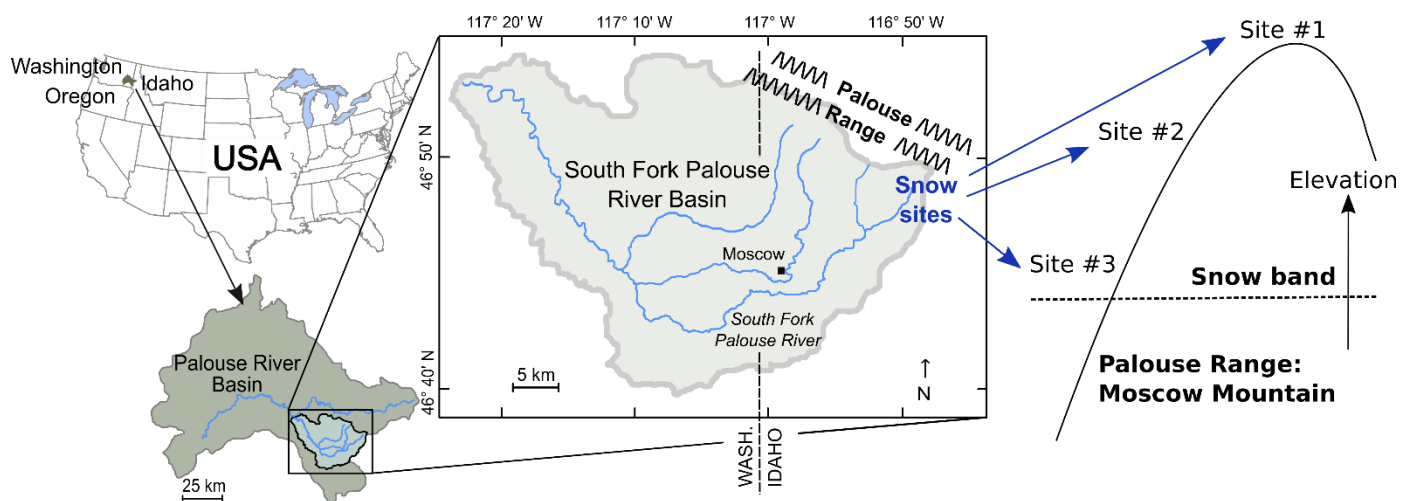

Figure 1. Study area location in the Palouse Range of the South Fork Palouse River Basin, northern Idaho, USA. Snow sampling network consisted of three sample locations within the primary snow band of Moscow Mountain.

Snowpack is a dynamic reservoir of water storage [35–37], where the physical and isotopic properties of a snowpack evolve, or age, from the initial retention of ground snow through to the final sublimation and melt [16,35,38–40]. The aging of a snowpack has a strong influence on the isotopic composition, particularly the redistribution of isotope signals within a snowpack [18,20,40–42]. Migration of water and vapor in a snowpack will occur with sublimation/condensation and evaporation/melt/freeze that will alter the internal distribution of isotope signals and subsequent snowmelt isotopic signals [20,27,41,43–45]. Melting of upper layers will produce isotopically different water that percolates through the snowpack and may refreeze at lower layers or exit the snowpack through the seasonal cycle [20,40,43,46]. Snowmelt isotope signals will vary with snow inputs and aging of the snowpack from accumulation through final melt and produce seasonally variable runoff isotope signals [16,19–21,27,41,44,46–54]. Additionally, these internal changes in snowpack isotope signals and subsequent snowmelt and runoff isotope signals can vary across a landscape because of temperature and insolation differences from elevation or orientation [45,55,56]. The evolution of the snowpack at different elevations in the study area likely contributes different snowmelt/runoff isotope signals to the surface-water and groundwater systems fed by this mountain snowpack reservoir.

2. Study Area Climate and Precipitation Isotope Signals

To examine the evolution of the snowpack for evaluating snowmelt and runoff isotope signals, a multi-elevation sampling network was established in the Palouse Range of north-central Idaho, USA (Figure 1). The region's climate is driven by its proximity to the Pacific Ocean and the northern Rocky Mountains, which produces a winter maritime climate and a summer continental climate [57–60]. Annually, this basin receives approximately 60 cm of precipitation (water equivalent), including 126 cm of snowfall [61]. The Palouse Range snowpack averages a snow-water equivalent of 50 cm at its highest elevations [62]. The snowpack will develop in late fall and typically last until late spring. Ephemeral

creeks will respond to snowmelt and precipitation in winter/spring and may contain flow into summer. These creeks, along with subsurface water, feed downgradient intermittent and perennial creeks along with providing recharge to the local aquifer system of the basin [31,32,63,64]. The hydrologic reservoir and recharge source that is the Palouse Range snowpack has produced variable isotope signals in connected surface-water and groundwater systems [31–33,64].

Precipitation isotope values for the region were predicted to range from strongly depleted winter values (e.g., January values of −169 to −133‰ for δ^2H and −22 to −13‰ for δ^{18}O) to relatively enriched summer rainfall (e.g., July values of −103 to −78‰ for δ^2H and −14 to −8‰ for δ^{18}O) [65]. This seasonal contrast in precipitation isotope values results from changes in the northern Pacific jet stream that seasonally shifts vapor sources and precipitation patterns across the region [60,66–69]. These shifts result in relatively dry summers with isotopically enriched late spring, summer, or fall rainfall and isotopically depleted and dominant winter/spring precipitation [70–73]. Along with these seasonal changes in isotope signals and precipitation patterns, d-excess typically is lower in the warmer summer/fall precipitation and higher in the winter precipitation [71,74,75].

3. Sample Collection and Data Analysis

3.1. Sampling Sites

As part of a larger study examining water isotopes across the basin [31–33], three Palouse Range sites were chosen for sampling of the snowpack and snowmelt in the primary snow band (Figures 1 and 2) where snowfall typically occurs from late November into April. Sites were chosen with glade-like characteristics that would minimize forest effects and allow for snow accumulation in an open-field setting. The sites range in elevation from 1430 m NAVD88 at Site #1, 1300 m at Site #2, to 1190 m at Site #3. As described in Behrens et al. [31], a snowpack sampling transect was established at each site to allow for interval trenching and collection of snow as a composite sample (full depth of the snowpack) and samples from the top, middle, and base layers of the snowpack. A snowmelt collector consisting of a 30-cm funnel pan with collection pipe and sampling tube, was installed adjacent to each snowpack transect [31]. During sampling, the density of the three sampling layers was determined through insertion and removal of a 160-cm^3 tube (30 cm length × 2.5 cm diameter) that was weighed with a hanging scale (snowpack density = snow weight/tube volume [76]). All isotope samples were collected and stored for minimization of atmospheric influence (vacuum-sealed bags for snow, no headspace in glass containers with polyseal caps for water). All isotope samples were analyzed at Washington State University with a Los Gatos Research Liquid Water Isotope Analyzer (instrument precision was ±0.25‰ for δ^2H and ±0.05‰ for δ^{18}O). Sampling frequency was monthly from December through February, biweekly in March, and weekly from April until the end of sampling. Snow was present at the sites until April 24 (site #3), May 8 (#2), and May 29 (Site #1). After the loss of the snowpack at each site, rainfall was collected from the snowmelt collectors until June 27. Ephemeral creeks (upper (A), middle (B), and lower (C) ephemeral creeks) located between Sites #2 and #3 (Figure 2) were sampled from March through June when runoff was accessible. The ephemeral creeks consist of small drainages <1 m in width and are first order streams in the upper portion of the watershed.
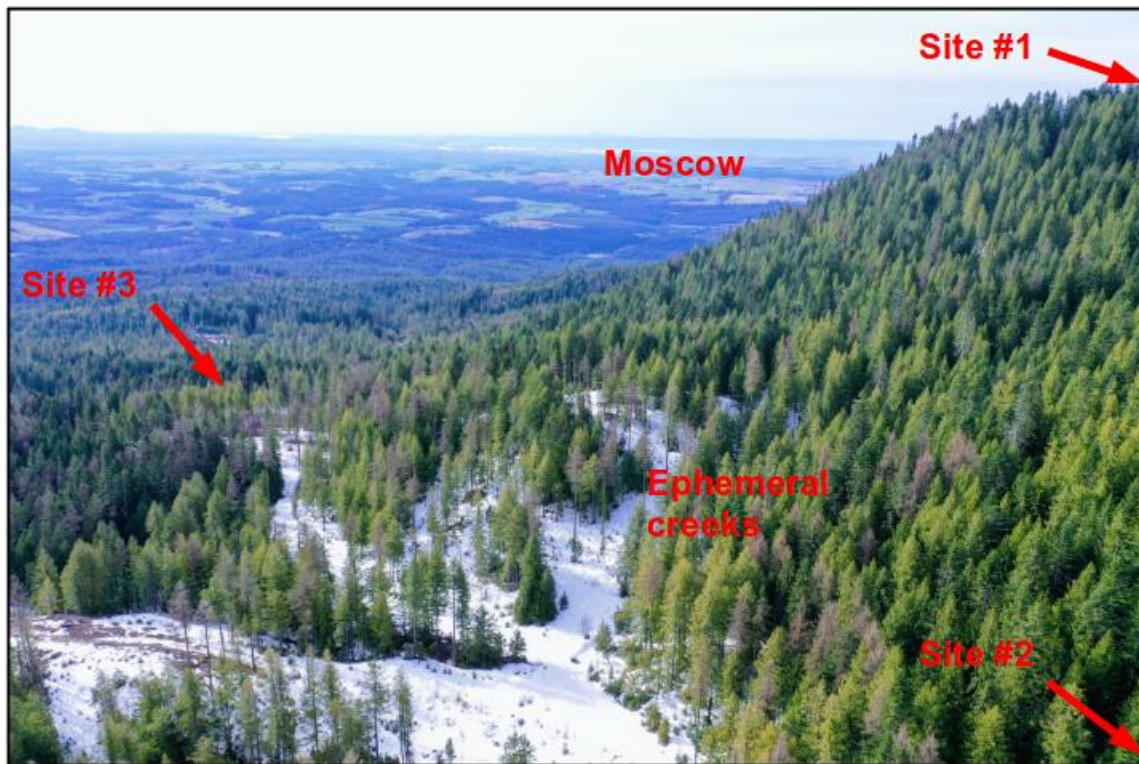
Figure 2. Sample collection locations along the eastern Palouse Range from a drone view looking towards Moscow, Idaho, USA.

3.2. Snow Density and Isotope Trendlines

The results of the study were compared through seasonal shifts (trends) in snow density and δ^2H and δ^{18}O values of snow, snowmelt, and ephemeral creek water. Snow density values were compared by elevation and layer against time to evaluate the physical alteration of the snowpack with aging. Linear regression trendlines (meteoric water lines) of composite isotope values were used to evaluate isotopic shifts by elevation through changes in trendline slope. Density and δ^{18}O trendlines were compared to evaluate the influence of snowpack aging on the isotope signal of the snowpack layers and redistribution of the isotope signals within the snowpack. Trendlines of layer values were used to evaluate shifts in each layer and expected snowmelt isotope signal from the release point (base layer). R values of the trendlines are provided to indicate strength and variability of the correlation (positively or negatively linear) for the trend direction. The goal of the linear regression trendline is to indicate an overall increase or decrease with the seasonal transition from winter to spring or the aging of the snowpack.

4. Results

Samples collected from the snow band of the Palouse Range in 2019–2020 produced a range of δ^2H and δ^{18}O values (Figure 3) that indicate highly variable isotope signals: snowpack values ranged from -130 to -75‰ for δ^2H and -18 to -10.5‰ for δ^{18}O and snowmelt values ranged from -120 to -90‰ for δ^2H and from -16.5 to -12‰ for δ^{18}O. With the transition of snowmelt to spring runoff, the range of isotope values decreased to -107 to -104‰ for δ^2H and -15.5 to -14.5‰ for δ^{18}O in the three ephemeral creeks. The range of snowpack isotope values highlights the variability of the snowpack isotope distribution throughout the winter–spring period, which does not directly translate to snowmelt and runoff. However, the transition to spring runoff did produce a relatively consistent springtime isotope signal in the runoff that fed the ephemeral creeks. The range of snowpack isotope signals indicates limited influence of elevation with the lowest elevation site recording the most depleted isotope signal, but the highest elevation site

recording the lowest median isotope value (median $\delta^{18}O$ values of -14.7, -14.1, and $-14.3‰$ for Sites #1–3, respectively). Site #2 had the largest field for snow accumulation, which may account for the more enriched isotope signals in the snowpack because of greater insolation and sublimation/evaporation.
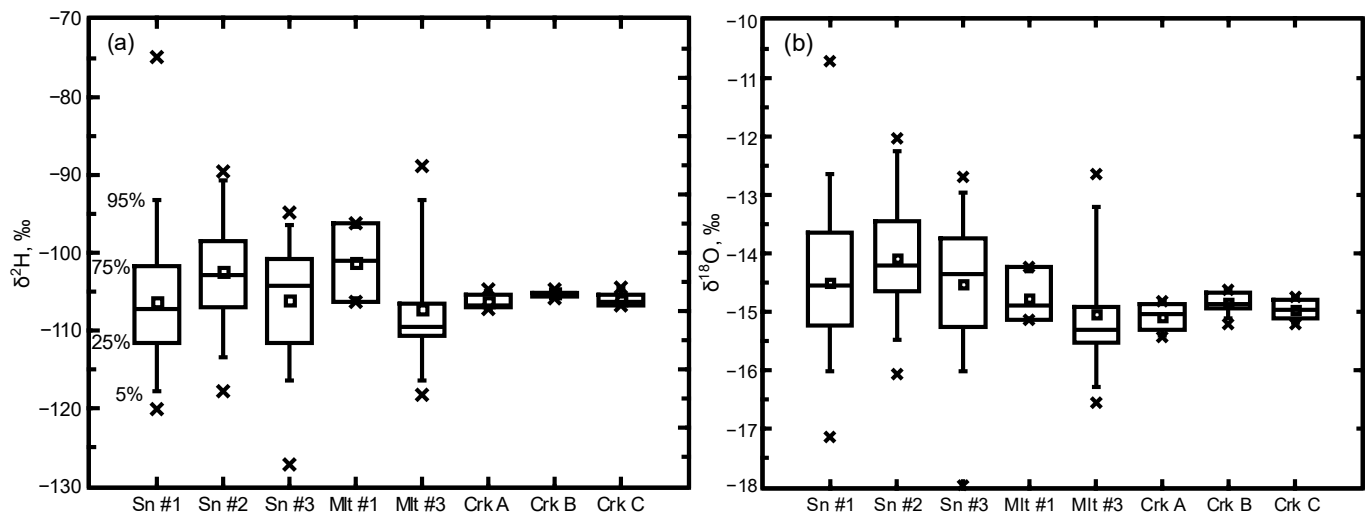

Figure 3. Distribution of δ^2H (**a**) and $\delta^{18}O$ (**b**) for snowpack (Sn), snowmelt (Mlt), and ephemeral creeks (Crk) in the study area. Boxplots indicate the median, mean (□), interquartile range (25% to 75%), and whisker range of 5% to 95% along with outliers (×).

An examination of the snowpack composite δ^2H and $\delta^{18}O$ values collected from each site indicate a relatively similar grouping along a meteoric water line (Figure 4). Individual trendlines for Site #2 and Site #3 indicate a decrease in slope compared to Site #1, primarily because of outliers at Site #2 and Site #3. These outliers were collected during the same sample period in late March and do not appear to be reflective of the local meteoric water lines for the snowpack at these sites. Removal of these two outliers results in trendlines of similar slope for all three sites (7.2, 6.8, and 6.6, respectively for Sites #1–3), although there are slightly lower slopes for lower elevation sites. This decreasing slope with elevation is reflective of greater evaporation given warmer temperatures at the lower elevations. The range of δ^2H and $\delta^{18}O$ values of the composite snowpack samples corresponds to predicted values of Bowen [65] for northern Idaho, although the snowpack did not contain the strongly depleted winter values (e.g., $\delta^{18}O$ values $< -20‰$) of Bowen's isoscapes.
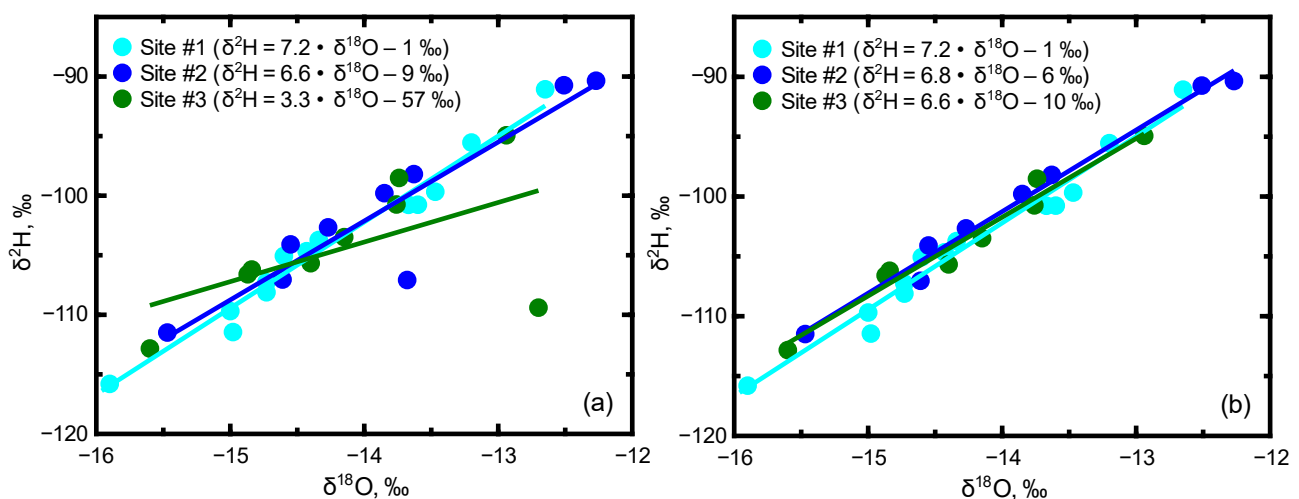

Figure 4. Linear regression trendlines (meteoric water lines) of δ^2H and $\delta^{18}O$ for snowpack composite samples collected at the three study sites. Outliers shown in (**a**) were removed to produce (**b**).

4.1. Snowpack Depth and Density

The range of isotope values for the snowpack, snowmelt, and ephemeral creeks occurred during a relatively average year for snowpack accumulation. The 2019–2020 snowpack at the SNOTEL site and the adjacent Site #1 (located in the same field area) were larger (160 cm peak) than the 30-year (1981–2010) average of 140 cm [62], but the 2019–2020 snowpack lasted a relatively similar duration compared to the 30-year average (Figure 5). The lowest elevation site (#3) produced a similar accumulation trend compared to Site #1, but the mid-elevation site (#2) indicated a later accumulation peak, although an expected snowpack duration between the higher and lower elevation sites. The larger open field quality of Site #2 appears to have delayed peak accumulation that may correlate to the relatively more enriched isotope signals (Figure 3).
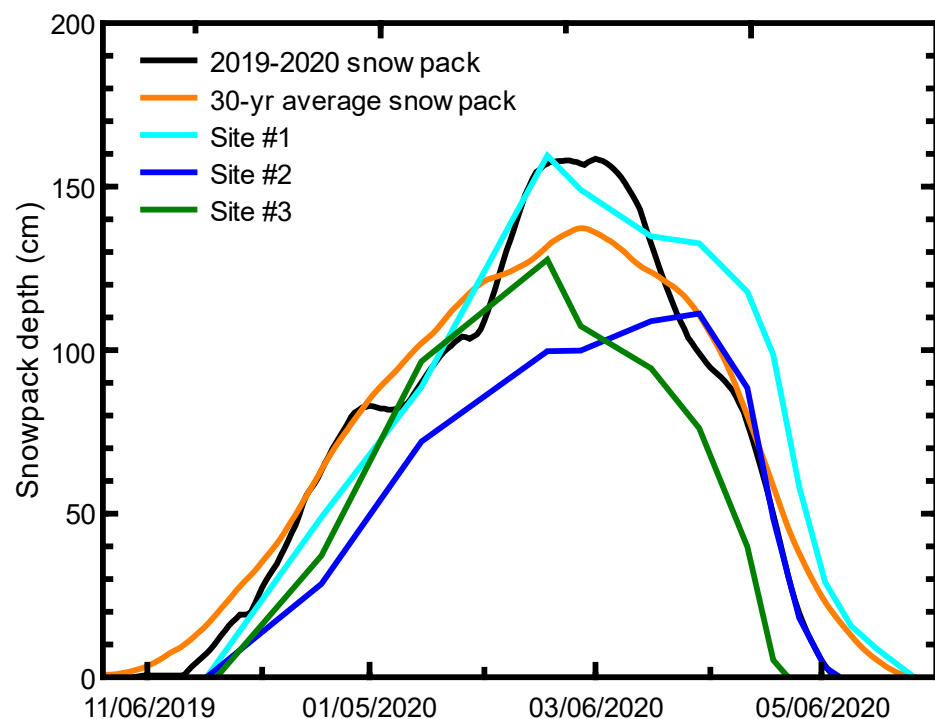

Figure 5. Snowpack depth for 2019–2020 and average snowpack depth, 1981–2010, for the Natural Resources and Conservation Service snow telemetry site at Moscow Mountain (site #989) [62] along with trendlines of snowpack-depth measurements at the three study sites (#1–3).

Linear trends in density of the snowpack layers at the three study sites indicate the highest densities and largest temporal increases in density at Site #1 (Figure 6), which is expected given the higher elevation, greater snowfall, and longer duration of the snowpack at this site (Figure 5). Sites #2 and #3 indicated overall smaller snowpack densities and variable density trends between layers (Figure 6). The density trends of the base layers at Site #2 and #3 were similar as opposed to the greater density increase in the base layer of Site #1. The greater snowfall (physical mass overlying the base layer) and longer duration (longer melt–refreeze sequence) of the snowpack at Site #1 likely allowed for increasing density in the base layer that also produced the sharper increasing density trend in all layers at this site. The difference in snowpack accumulation between Site #2 and #3 (Figure 5) resulted in Site #3 having slightly higher densities although similar temporal trends (slope) in the base layer density (Figure 6). At Site #2 and #3, the variability of isotope signals (Figures 3 and 4), snowpack accumulation (Figure 5), and greater temperature influence were apparent in the variable strength (R values) of the linear trend for density of all layers. The difference in physical and isotopic characteristics and trends for the snowpack at Site #2 highlight the effect of orientation and landscape given the larger clearing for

snow accumulation that made it more available to insolation and wind effects. The greater temperature influence and corresponding shorter duration of the snowpack at the lower elevation Site #3 increased the variability of the snowpack density trends (R = 0.3 to 0.7) and produced the lowest meteoric water line slope (Figure 4) indicative of greater evaporation.
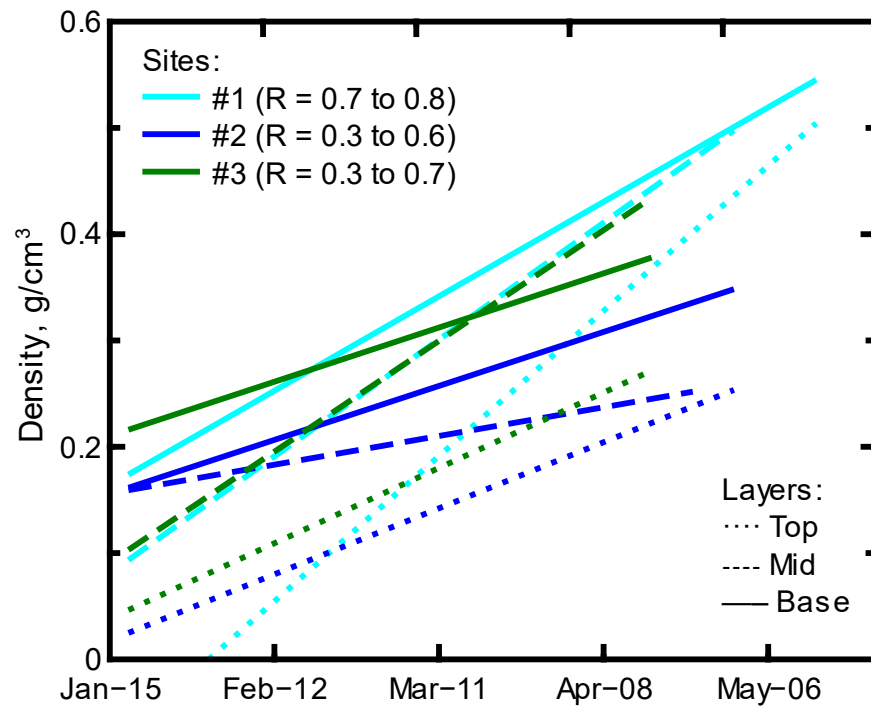

Figure 6. Linear regression trendlines of the density data collected for each layer at the three study sites.

4.2. Isotope Signals in the Snowpack Layers

The aging of the snowpack from accumulation through melt that produced variable densities by layer also produced variable isotope signals by layer (Figure 7). Similar to the density trends, the temporal relationships between δ^2H and δ^{18}O indicate variable changes between layers at each site. Isotope trendlines for the snowpack layers at Site #1 indicate a decreasing slope from the top layer to base layer. This isotope signal evolution with depth was not as apparent at the lower elevation sites (#2 and #3), but the base layer at each of these sites had the lowest trendline slope. These base layers represent the earliest or oldest snow that also receives melt from subsequent layers (accumulation of the evaporation/sublimation signal as melt residual). The rotation of the layer trendlines (lower slope) from top to base layer reflect the aging of the older snow or middle and base layers. An examination of δ^{18}O vs. time (Figure 7) indicates an enrichment trend in the base layer with aging of the snowpack. Top layers at Site #1 and #3 indicate the most depleted initial δ^{18}O values that also became more enriched with time and became the most enriched values of all the layers. The mid-elevation Site #2 had similar trends in δ^{18}O values for the top and base layers, and sampling of the middle layer captured a trend similar to that seen in the top layer, but at a more depleted signal.
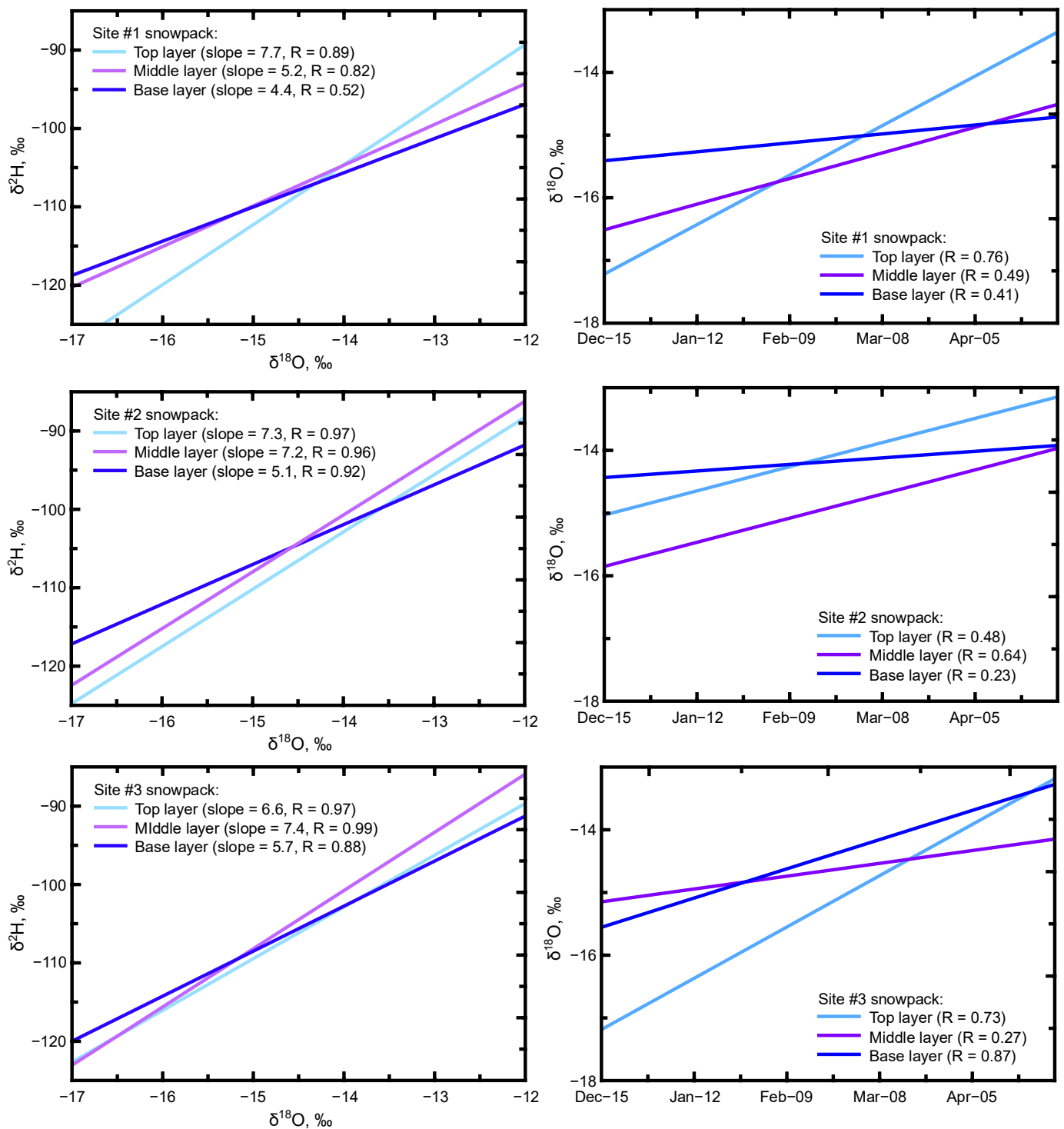
Figure 7. Linear regression trendlines of δ^2H and $\delta^{18}O$ and $\delta^{18}O$ with time for the snowpack sampling sites by layer.

4.3. Deuterium Excess

While the δ^2H and $\delta^{18}O$ relationship can indicate the effects of evaporation/sublimation, the second order isotopic parameter of d-excess can indicate vapor re-circulation/transport or the conditions in an evolving system such as a snowpack. D-excess is a function of the isotopic composition of hydrogen (δ^2H) and oxygen ($\delta^{18}O$) in water (d-excess = $\delta^2H - 8 \times \delta^{18}O$) [77], where the d-excess will be altered during circulation because of diffusivity differences from differences in molecular weight (e.g., $^1H^2H^{16}O = 19$ g·mol/mol compared to $^1H^1H^{18}O = 20$ g·mol/mol).

D-excess responds to humidity/evaporation changes at the vapor source and with precipitation (subcloud evaporation) [74,75,78]. Redistribution in a system, such as through the movement of vapor and melt in a snowpack, can produce additional isotope signal differences as melt water and water vapor migrate through a snowpack and undergo freezing (re-deposition) or are lost from the system. Snowfall in the study area is expected to have a relatively large d-excess that is greater with elevation [75], which will be altered with aging of the snowpack. The linear trends of d-excess with time (Figure 8) indicate an overall decrease in d-excess in all layers at all three snowpack sites. This trend is inverse to the enrichment trend in $\delta^{18}O$ with time (Figure 7). This d-excess trend is reflective of vapor and melt migration in the snowpack during aging, which corresponds to the enrichment trend of $\delta^{18}O$.
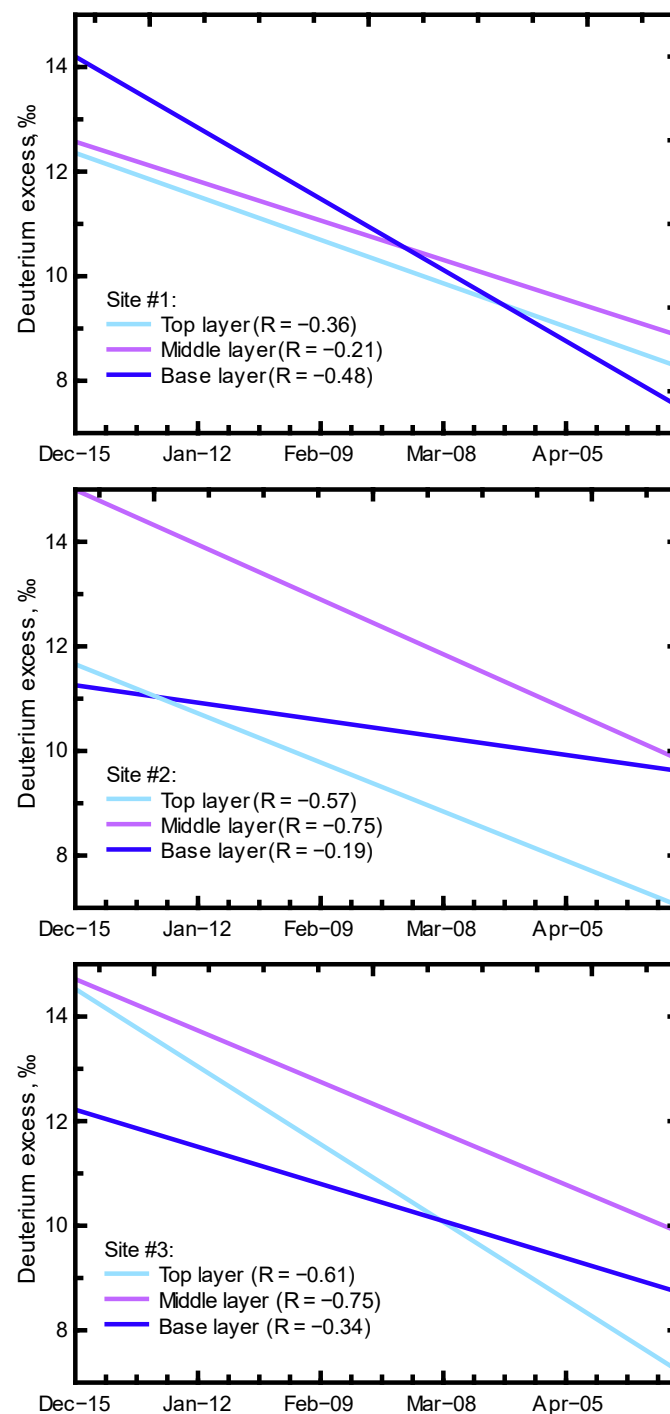

Figure 8. Linear regression trendlines of deuterium excess with time at the three snowpack sites.

The decreasing d-excess trend is not the same for each layer at each site or between sites, indicating different internal signals from the snow/vapor/melt/freeze/loss distribution of the water. D-excess values at Site #1 indicated similar temporal trends, although with a larger decrease in d-excess in the base layer. This initially larger d-excess and greater decrease in d-excess in the base layer of Site #1 is expected given the duration of the snowpack where early winter, upper elevation snow contained a relatively large d-excess value that decreased with later distribution of melt and loss as snowmelt from the snowpack. A similar base layer d-excess trend was not present at the lower elevation sites, which reflects differing evolution of the snowpack at these sites because of the different temperature regimes. The lower initial d-excess and lower slope of the d-excess trend in the base layers of Site #2 and #3 indicate differences in base layer water accumulations and release as snowmelt. This difference in the base layers of the lower elevation sites aligns with the greater variability in δ^2H and $\delta^{18}O$ values recorded for the snowmelt collected at Site #3 compared to Site #1.

4.4. Persistence and Variability of the Snowmelt and Runoff Isotope Signals

The aging of the snowpack produced variable snowpack isotope signals but less variable signals in the subsequent snowmelt and ephemeral creeks (Figure 3). The wide range of snowpack isotope values (e.g., $\delta^{18}O$ range of -18 to $-10.5‰$) translated to a slightly smaller range of snowmelt isotope values (e.g., $\delta^{18}O$ range of -16.5 to $-12‰$) and a very limited range of relatively depleted isotope values in the springtime, ephemeral creeks (e.g., $\delta^{18}O$ range of -15.5 to $-14.5‰$). The compression of the isotope signal from snowpack $\rightarrow$ snowmelt $\rightarrow$ runoff indicates substantial loss of snowpack water through evaporation/sublimation and early (winter) melt that was visible in the enrichment of the snowpack isotope signals (Figure 7) and the alteration of d-excess values (Figure 8) from winter through spring. The snowpack-to-snowmelt evolution produced a consistent, relatively depleted isotope signal for runoff in the upper watershed, ephemeral creeks. This consistent isotope signal in the springtime ephemeral creeks was not influenced by subsequent enriched rainfall (Figure 9). The compressed range of relatively depleted isotope signals in the springtime ephemeral creeks suggests a strong influence from early melt (winter melt) because of the relative weighting of the creek water towards the depleted portion of the snowpack and snowmelt δ^2H and $\delta^{18}O$ range of values.
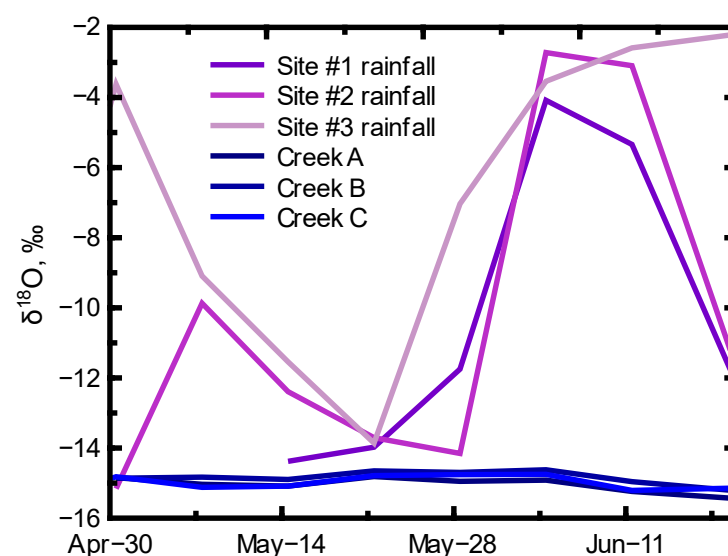

Figure 9. Temporal trends of $\delta^{18}O$ values for spring rainfall collected at the three snowpack sampling locations (Sites #1–3) and the three (A, B, and C) ephemeral creeks located between sites #2 and #3.

Given the dominance of the depleted isotope signal in ephemeral creek runoff ($\sim -15‰$ for $\delta^{18}O$, Figure 9) and no discernible difference in runoff isotope signals between the

three ephemeral creeks over the springtime sampling period, it appears the snowpack → snowmelt → runoff process is dominated by high elevation and/or early melt with a sufficient diversity of pathways to create a steady isotopic signal for upper watershed, creek water. Base layer isotope signals of Site #1 (δ^{18}O median of −14.9‰) and Site #2 (δ^{18}O median of −14.2‰) along with a Site #1 snowmelt median of −14.9‰ (Figure 3) suggest large contributions of upper elevation snowmelt to the ephemeral creek runoff. However, the wide range of snowmelt values at Site #3 (Figure 3, δ^{18}O median of −15.3‰) indicates the availability of relatively depleted runoff at lower elevations. Such a range of snowmelt and runoff isotope signals parallels the wide range of isotope signals found in a downgradient perennial creek (Crumarine Creek: range of −17.7 to −13.7‰ (mean = −15.2‰) by Sanchez-Murillo et al. [63] and isotope signals in two downgradient, shallow groundwater wells (range of −16.0 to −14.8‰ (well 9) and −15.6 to −14.6‰ (well 14)) by Candel et al. [64] (Figure 10). The wide range of snowpack and snowmelt isotope signals can produce a consistent isotope signal for high elevation, ephemeral creek water, but other pathways (e.g., snowmelt infiltration/percolation = subsurface water) can allow for substantial variation in isotope signals in lower elevation surface-water and groundwater systems (Figure 10).
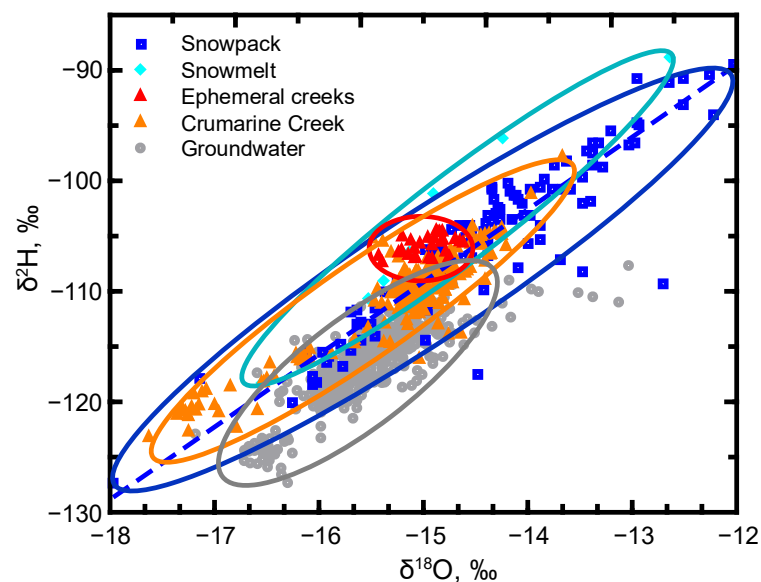

Figure 10. Groupings of δ^2H and δ^{18}O values indicative of the evolution and variability of the isotope signals from snowpack and snowmelt to local surface-water and groundwater systems. Crumarine Creek and groundwater values are from Sanchez-Murillo et al. [63] and Candel et al. [64], respectively.

5. Conclusions

As a snowpack ages, δ^2H and δ^{18}O values will vary according to the inputted snow values and will evolve in their distribution within the snowpack as melt moves through and out of the snowpack. An examination of δ^2H and δ^{18}O values for snowpack, snowmelt, and ephemeral creek water in a snow-dominated basin of northern Idaho indicated an evolution of δ^2H and δ^{18}O values from variably depleted snowpack to enriched snowmelt and relatively consistent isotope signals in springtime ephemeral creeks. Spatial and temperature influences on the winter/spring snowpack produced an isotope range of −130 to −75‰ for δ^2H and −18 to −10.5‰ for δ^{18}O, which produced snowmelt values ranging −120 to −90‰ for δ^2H and −16.5 to −12‰ for δ^{18}O. With the transport of snowmelt to springtime ephemeral creeks, the isotope values compressed to −107 to −104‰ for δ^2H and −15.5 to −14.5‰ for δ^{18}O. The aging of the snowpack produced increasing densities in the base, middle, and top layers along with a corresponding temporal enrichment of isotope values. However, the snowpack produced a variable pattern of isotope enrichment at the three different sampling elevations. The highest elevation site indicated the least

enrichment of the isotope signal in the snowpack base layer, and the lowest elevation site indicated the strongest enrichment of the isotope signal in the snowpack base layer. The linear trends of d-excess with time indicate an overall decrease in d-excess in all layers at all three snowpack sites, which was inverse to the enrichment trend in δ^{18}O with time. The decreasing d-excess trend was not the same for each layer at each site, or between sites, indicating different internal signals from snow/vapor/melt/freeze/loss distribution of the water. The d-excess trends are reflective of vapor and melt migration in the snowpack, which is a substantial influence on isotope signals during snowpack aging and can produce a relatively consistent temporal trend of enriched isotope signals.

The accumulation of the snowpack provides a dominant water source for infiltration and runoff from the mountain system, which provides water to the creek system and recharge to the local aquifer system. The evolution of the isotope signal from snowpack to snowmelt to ephemeral creek aligns with some groundwater isotope signals found in the lower elevations along the mountain front, but more strongly depleted isotope signals have been found in other groundwater and perennial creek water in the same area. It is likely that winter melt (early depleted signal) is a primary contributor to creeks and groundwater, but this early melt was not well captured by the current study. However, the snowpack and snowmelt isotope signals recorded for this study captured the evolution of and variation in isotope signals that feed the surface-water and groundwater systems of the basin.

References

1. Simpkins, G. Snow-Related Water Woes. *Nat. Clim Chang.* **2018**, *8*, 945. [CrossRef]
2. Viviroli, D.; Dürr, H.H.; Messerli, B.; Meybeck, M.; Weingartner, R. Mountains of the World, Water Towers for Humanity: Typology, Mapping, and Global Significance. *Water Resour. Res.* **2007**, *43*, W07447. [CrossRef]
3. Rodhe, A. Chapter 12—Snowmelt-Dominated Systems. In *Isotope Tracers in Catchment Hydrology*; Kendall, C., McDonnell, J.J., Eds.; Elsevier: Amsterdam, The Netherlands, 1998; pp. 391–433. ISBN 978-0-444-81546-0.
4. Siirila-Woodburn, E.R.; Rhoades, A.M.; Hatchett, B.J.; Huning, L.S.; Szinai, J.; Tague, C.; Nico, P.S.; Feldman, D.R.; Jones, A.D.; Collins, W.D.; et al. A Low-to-No Snow Future and Its Impacts on Water Resources in the Western United States. *Nat. Rev. Earth Environ.* **2021**, *2*, 800–819. [CrossRef]
5. Fayad, A.; Gascoin, S.; Faour, G.; López-Moreno, J.I.; Drapeau, L.; Page, M.L.; Escadafal, R. Snow Hydrology in Mediterranean Mountain Regions: A Review. *J. Hydrol.* **2017**, *551*, 374–396. [CrossRef]
6. Armstrong, R.L.; Rittger, K.; Brodzik, M.J.; Racoviteanu, A.; Barrett, A.P.; Khalsa, S.-J.S.; Raup, B.; Hill, A.F.; Khan, A.L.; Wilson, A.M.; et al. Runoff from Glacier Ice and Seasonal Snow in High Asia: Separating Melt Water Sources in River Flow. *Reg. Environ. Chang.* **2019**, *19*, 1249–1261. [CrossRef]
7. Araguás-Araguás, L.; Froehlich, K.; Rozanski, K. Deuterium and Oxygen-18 Isotope Composition of Precipitation and Atmospheric Moisture. *Hydrol. Processes* **2000**, *14*, 1341–1355. [CrossRef]

8. Gonfiantini, R.; Frohlich, K.; Araguas-Araguas, L.; Rozanski, K. Isotopes in Groundwater Hydrology. In *Isotope Tracers in Catchment Hydrology*; Elsevier Science B.V.: Amsterdam, The Netherlands, 1998; pp. 203–246. ISBN 0-444-50155-X.

9. Klaus, J.; McDonnell, J.J. Hydrograph Separation Using Stable Isotopes: Review and Evaluation. *J. Hydrol.* **2013**, *505*, 47–64. [CrossRef]

10. Rodgers, P.; Soulsby, C.; Waldron, S. Stable Isotope Tracers as Diagnostic Tools in Upscaling Flow Path Understanding and Residence Time Estimates in a Mountainous Mesoscale Catchment. *Hydrol. Processes* **2005**, *19*, 2291–2307. [CrossRef]

11. Maule, C.P.; Chanasyk, D.S.; Muehlenbachs, K. Isotopic Determination of Snow-Water Contribution to Soil Water and Groundwater. *J. Hydrol.* **1994**, *155*, 73–91. [CrossRef]

12. Vogel, T.; Sanda, M.; Dusek, J.; Dohnal, M.; Votrubova, J. Using Oxygen-18 to Study the Role of Preferential Flow in the Formation of Hillslope Runoff. *Vadose Zone J.* **2010**, *9*, 252–259. [CrossRef]

13. Maulé, C.P.; Stein, J. Hydrologic Flow Path Definition and Partitioning of Spring Meltwater. *Water Resour. Res.* **1990**, *26*, 2959–2970. [CrossRef]

14. Yuan, F.; Sheng, Y.; Yao, T.; Fan, C.; Li, J.; Zhao, H.; Lei, Y. Evaporative Enrichment of Oxygen-18 and Deuterium in Lake Waters on the Tibetan Plateau. *J. Paleolimnol.* **2011**, *46*, 291–307. [CrossRef]

15. Penna, D.; Ahmad, M.; Birks, S.J.; Bouchaou, L.; Brenčič, M.; Butt, S.; Holko, L.; Jeelani, G.; Martínez, D.E.; Melikadze, G.; et al. A New Method of Snowmelt Sampling for Water Stable Isotopes. *Hydrol. Processes* **2014**, *28*, 5637–5644. [CrossRef]

16. Beria, H.; Larsen, J.R.; Ceperley, N.C.; Michelon, A.; Vennemann, T.; Schaefli, B. Understanding Snow Hydrological Processes through the Lens of Stable Water Isotopes. *Wiley Interdiscip. Rev. Water* **2018**, *5*, e1311. [CrossRef]

17. Cooper, L.W.; Solis, C.; Kane, D.L.; Hinzman, L.D. Application of Oxygen-18 Tracer Techniques to Arctic Hydrological Processes. *Arct. Alp. Res.* **1993**, *25*, 247–255. [CrossRef]

18. Cooper, L.W. Chapter 4—Isotopic Fractionation in Snow Cover. In *Isotope Tracers in Catchment Hydrology*; Kendall, C., McDonnell, J.J., Eds.; Elsevier: Amsterdam, The Netherlands, 1998; pp. 119–136. ISBN 978-0-444-81546-0.

19. Laudon, H.; Hemond, H.F.; Krouse, R.; Bishop, K.H. Oxygen 18 Fractionation during Snowmelt: Implications for Spring Flood Hydrograph Separation. *Water Resour. Res.* **2002**, *38*, 1258. [CrossRef]

20. Taylor, S.; Feng, X.; Kirchner, J.W.; Osterhuber, R.; Klaue, B.; Renshaw, C.E. Isotopic Evolution of a Seasonal Snowpack and Its Melt. *Water Resour. Res.* **2001**, *37*, 759–769. [CrossRef]

21. Laudon, H.; Seibert, J.; Köhler, S.; Bishop, K. Hydrological Flow Paths during Snowmelt: Congruence between Hydrometric Measurements and Oxygen 18 in Meltwater, Soil Water, and Runoff. *Water Resour. Res.* **2004**, *40*, W03102. [CrossRef]

22. Schmieder, J.; Garvelmann, J.; Marke, T.; Strasser, U. Spatio-Temporal Tracer Variability in the Glacier Melt End-Member—How Does It Affect Hydrograph Separation Results? *Hydrol. Processes* **2018**, *32*, 1828–1843. [CrossRef]

23. Ala-aho, P.; Tetzlaff, D.; McNamara, J.P.; Laudon, H.; Kormos, P.; Soulsby, C. Modeling the Isotopic Evolution of Snowpack and Snowmelt: Testing a Spatially Distributed Parsimonious Approach. *Water Resour. Res.* **2017**, *53*, 5813–5830. [CrossRef]

24. Laudon, H.; Sjöblom, V.; Buffam, I.; Seibert, J.; Mörth, M. The Role of Catchment Scale and Landscape Characteristics for Runoff Generation of Boreal Streams. *J. Hydrol.* **2007**, *344*, 198–209. [CrossRef]

25. N'da, A.B.; Bouchaou, L.; Reichert, B.; Hanich, L.; Ait Brahim, Y.; Chehbouni, A.; Beraaouz, E.H.; Michelot, J.-L. Isotopic Signatures for the Assessment of Snow Water Resources in the Moroccan High Atlas Mountains: Contribution to Surface and Groundwater Recharge. *Env. Earth Sci.* **2016**, *75*, 755. [CrossRef]

26. Jeelani, G.; Bhat, N.A.; Shivanna, K. Use of Δ18O Tracer to Identify Stream and Spring Origins of a Mountainous Catchment: A Case Study from Liddar Watershed, Western Himalaya, India. *J. Hydrol.* **2010**, *393*, 257–264. [CrossRef]

27. Moser, H.; Stichler, W. Deuterium and Oxygen-18 Contents as an Index of the Properties of Snow Covers. *Int. Assoc. Hydrol. Sci.* **1974**, *114*, 122–135.

28. Zongxing, L.; Qi, F.; Wei, L.; Tingting, W.; Xiaoyan, G.; Zongjie, L.; Yan, G.; Yanhui, P.; Rui, G.; Bing, J.; et al. The Stable Isotope Evolution in Shiyi Glacier System during the Ablation Period in the North of Tibetan Plateau, China. *Quat. Int.* **2015**, *380–381*, 262–271. [CrossRef]

29. Winograd, I.J.; Riggs, A.C.; Coplen, T.B. The Relative Contributions of Summer and Cool-Season Precipitation to Groundwater Recharge, Spring Mountains, Nevada, USA. *Hydrogeol. J.* **1998**, *6*, 77–93. [CrossRef]

30. Jasechko, S.; Perrone, D.; Befus, K.M.; Bayani-Cardenas, M.; Ferguson, G.; Gleeson, T.; Luijendijk, E.; McDonnell, J.J.; Taylor, R.G.; Wada, Y.; et al. Global Aquifers Dominated by Fossil Groundwaters but Wells Vulnerable to Modern Contamination. *Nat. Geosci.* **2017**, *10*, 425–429. [CrossRef]

31. Behrens, D.; Langman, J.B.; Brooks, E.S.; Boll, J.; Waynant, K.; Moberly, J.G.; Dodd, J.K.; Dodd, J.W. Tracing $\delta^{18}O$ and $\delta^{2}H$ in Source Waters and Recharge Pathways of a Fractured-Basalt and Interbedded-Sediment Aquifer, Columbia River Flood Basalt Province. *Geosciences* **2021**, *11*, 400. [CrossRef]

32. Duckett, K.A.; Langman, J.B.; Bush, J.H.; Brooks, E.S.; Dunlap, P.; Welker, J.M. Isotopic Discrimination of Aquifer Recharge Sources, Subsystem Connectivity and Flow Patterns in the South Fork Palouse River Basin, Idaho and Washington, USA. *Hydrology* **2019**, *6*, 15. [CrossRef]

33. Duckett, K.A.; Langman, J.B.; Bush, J.H.; Brooks, E.S.; Dunlap, P.; Stanley, J.R. Noble Gases, Dead Carbon, and Reinterpretation of Groundwater Ages and Travel Time in Local Aquifers of the Columbia River Basalt Group. *J. Hydrol.* **2020**, *581*, 124400. [CrossRef]

34. Medici, G.; Engdahl, N.B.; Langman, J.B. A Basin-Scale Groundwater Flow Model of the Columbia Plateau Regional Aquifer System in the Palouse (USA): Insights for Aquifer Vulnerability Assessment. *Int. J. Environ. Res* **2021**, *15*, 299–312. [CrossRef]

35. Sturm, M. White Water: Fifty Years of Snow Research in WRR and the Outlook for the Future. *Water Resour. Res.* **2015**, *51*, 4948–4965. [CrossRef]

36. Cohen, J.S.; Zeff, H.B.; Herman, J.D. Adaptation of Multiobjective Reservoir Operations to Snowpack Decline in the Western United States. *J. Water Resour. Plan. Manag.* **2020**, *146*, 04020091. [CrossRef]

37. Rhoades, A.M.; Jones, A.D.; Ullrich, P.A. The Changing Character of the California Sierra Nevada as a Natural Reservoir. *Geophys. Res. Lett.* **2018**, *45*, 13,008–13,019. [CrossRef]

38. Viallon-Galinier, L.; Hagenmuller, P.; Lafaysse, M. Forcing and Evaluating Detailed Snow Cover Models with Stratigraphy Observations. *Cold Reg. Sci. Technol.* **2020**, *180*, 103163. [CrossRef]

39. Domine, F.; Morin, S.; Brun, E.; Lafaysse, M.; Carmagnola, C.M. Seasonal Evolution of Snow Permeability under Equi-Temperature and Temperature-Gradient Conditions. *Cryosphere* **2013**, *7*, 1915–1929. [CrossRef]

40. Lee, J.; Feng, X.; Faiia, A.M.; Posmentier, E.S.; Kirchner, J.W.; Osterhuber, R.; Taylor, S. Isotopic Evolution of a Seasonal Snowcover and Its Melt by Isotopic Exchange between Liquid Water and Ice. *Chem. Geol.* **2010**, *270*, 126–134. [CrossRef]

41. Earman, S.; Campbell, A.R.; Phillips, F.M.; Newman, B.D. Isotopic Exchange between Snow and Atmospheric Water Vapor: Estimation of the Snowmelt Component of Groundwater Recharge in the Southwestern United States. *J. Geophys. Res. Atmos.* **2006**, *111*, D09302. [CrossRef]

42. Kendall, C.; Caldwell, E.A. Chapter 2—Fundamentals of Isotope Geochemistry. In *Isotope Tracers in Catchment Hydrology*; Kendall, C., McDonnell, J.J., Eds.; Elsevier: Amsterdam, The Netherlands, 1998; ISBN 978-0-08-092915-6.

43. O'Neil, J.R. Hydrogen and Oxygen Isotope Fractionation between Ice and Water. *J. Phys. Chem.* **1968**, *72*, 3683–3684. [CrossRef]

44. Stichler, W.; Rauert, W.; Martinec, J. Environmental Isotope Studies of an Alpine Snowpack. *Hydrol. Res.* **1981**, *12*, 297–308. [CrossRef]

45. Dahlke, H.E.; Lyon, S.W. Early Melt Season Snowpack Isotopic Evolution in the Tarfala Valley, Northern Sweden. *Ann. Glaciol.* **2013**, *54*, 149–156. [CrossRef]

46. Dietermann, N.; Weiler, M. Spatial Distribution of Stable Water Isotopes in Alpine Snow Cover. *Hydrol. Earth Syst. Sci.* **2013**, *17*, 2657–2668. [CrossRef]

47. Hood, E.; Williams, M.; Cline, D. Sublimation from a Seasonal Snowpack at a Continental, Mid-Latitude Alpine Site. *Hydrol. Processes* **1999**, *13*, 1781–1797. [CrossRef]

48. Unnikrishna, P.V.; McDonnell, J.J.; Kendall, C. Isotope Variations in a Sierra Nevada Snowpack and Their Relation to Meltwater. *J. Hydrol.* **2002**, *260*, 38–57. [CrossRef]

49. Gustafson, J.R.; Brooks, P.D.; Molotch, N.P.; Veatch, W.C. Estimating Snow Sublimation Using Natural Chemical and Isotopic Tracers across a Gradient of Solar Radiation. *Water Resour. Res.* **2010**, *46*, W12511. [CrossRef]

50. Reba, M.L.; Pomeroy, J.; Marks, D.; Link, T.E. Estimating Surface Sublimation Losses from Snowpacks in a Mountain Catchment Using Eddy Covariance and Turbulent Transfer Calculations. *Hydrol. Processes* **2012**, *26*, 3699–3711. [CrossRef]

51. Shanley, J.B.; Kendall, C.; Albert, M.R.; Hardy, J.P. Chemical and Isotopic Evolution of a Layered Eastern U.S. Snowpack and Its Relation to Stream-Water Composition. In Proceedings of the International Association of Hydrological Sciences: Biogeochemistry of Seasonally Snow-Covered Catchments. Symposium during the XXI Assembly of the International Union of Geodesy and Geophysic, Boulder, CO, USA, 2–14 July 1995; Volume 228, pp. 329–338.

52. Soulsby, C.; Malcolm, R.; Helliwell, R.; Ferrier, R.C.; Jenkins, A. Isotope Hydrology of the Allt a' Mharcaidh Catchment, Cairngorms, Scotland: Implications for Hydrological Pathways and Residence Times. *Hydrol. Processes* **2000**, *14*, 747–762. [CrossRef]

53. Feng, X.; Taylor, S.; Renshaw, C.E.; Kirchner, J.W. Isotopic Evolution of Snowmelt 1. A Physically Based One-Dimensional Model. *Water Resour. Res.* **2002**, *38*, 1217. [CrossRef]

54. Carey, S.K.; Quinton, W.L. Evaluating Snowmelt Runoff Generation in a Discontinuous Permafrost Catchment Using Stable Isotope, Hydrochemical and Hydrometric Data. *Hydrol. Res.* **2004**, *35*, 309–324. [CrossRef]

55. Schmieder, J.; Hanzer, F.; Marke, T.; Garvelmann, J.; Warscher, M.; Kunstmann, H.; Strasser, U. The Importance of Snowmelt Spatiotemporal Variability for Isotope-Based Hydrograph Separation in a High-Elevation Catchment. *Hydrol. Earth Syst. Sci.* **2016**, *20*, 5015–5033. [CrossRef]

56. Evans, S.L.; Flores, A.N.; Heilig, A.; Kohn, M.J.; Marshall, H.-P.; McNamara, J.P. Isotopic Evidence for Lateral Flow and Diffusive Transport, but Not Sublimation, in a Sloped Seasonal Snowpack, Idaho, USA. *Geophys. Res. Lett.* **2016**, *43*, 3298–3306. [CrossRef]

57. Finklin, A.I. *Climate of Priest River Experimental Forest, Northern Idaho*; Gen. Tech. Rep. INT-159; US Department of Agriculture, Forest Service, Intermountain Forest and Range Experiment Station: Ogden, Utah, USA, 1983; Volume 159, 53p. [CrossRef]

58. Rutz, J.J.; Steenburgh, W.J.; Ralph, F.M. Climatological Characteristics of Atmospheric Rivers and Their Inland Penetration over the Western United States. *Mon. Weather Rev.* **2014**, *142*, 905–921. [CrossRef]

59. Hu, Q.; Feng, S. AMO- and ENSO-Driven Summertime Circulation and Precipitation Variations in North America. *J. Clim.* **2012**, *25*, 6477–6495. [CrossRef]

60. Neiman, P.J.; Ralph, F.M.; Wick, G.A.; Lundquist, J.D.; Dettinger, M.D. Meteorological Characteristics and Overland Precipitation Impacts of Atmospheric Rivers Affecting the West Coast of North America Based on Eight Years of SSM/I Satellite Observations. *J. Hydrometeor.* **2008**, *9*, 22–47. [CrossRef]

61. Western Regional Climate Center Cooperative Climatological Data Summaries, NOAA Cooperative Stations, Pullman Experimental Station-Climate Summary. Available online: https://wrcc.dri.edu/cgi-bin/cliMAIN.pl?id6152 (accessed on 9 January 2021).

62. Northwest River Forecast Center Temperature and Precipitation Monthly Means. Available online: https://www.nwrfc.noaa.gov/snow/snowplot.cgi?MSCI1 (accessed on 19 April 2021).

63. Sánchez-Murillo, R.; Brooks, E.S.; Elliot, W.J.; Boll, J. Isotope Hydrology and Baseflow Geochemistry in Natural and Human-Altered Watersheds in the Inland Pacific Northwest, USA. *Isot. Environ. Health Stud.* **2015**, *51*, 231–254. [CrossRef] [PubMed]

64. Candel, J.; Brooks, E.; Sánchez-Murillo, R.; Grader, G.; Dijksma, R. Identifying Groundwater Recharge Connections in the Moscow (USA) Sub-Basin Using Isotopic Tracers and a Soil Moisture Routing Model. *Hydrogeol. J.* **2016**, *24*, 1739–1751. [CrossRef]

65. Bowen, G.J. Statistical and Geostatistical Mapping of Precipitation Water Isotope Ratios. In *Isoscapes: Understanding Movement, Pattern, and Process on Earth through Isotope Mapping*; West, J.B., Bowen, G.J., Dawson, T.E., Tu, K.P., Eds.; Springer: Dordrecht, The Netherlands, 2010; pp. 139–160. ISBN 978-90-481-3354-3.

66. Ellis, A.W.; Barton, N.P. Characterizing the North Pacific Jet Stream for Understanding Historical Variability in Western United States Winter Precipitation. *Phys. Geogr.* **2012**, *33*, 105–128. [CrossRef]

67. Zhang, W.; Villarini, G. Uncovering the Role of the East Asian Jet Stream and Heterogeneities in Atmospheric Rivers Affecting the Western United States. *Proc. Natl. Acad. Sci. USA* **2018**, *115*, 891–896. [CrossRef]

68. Lackmann, G.M.; Gyakum, J.R. Heavy Cold-Season Precipitation in the Northwestern United States: Synoptic Climatology and an Analysis of the Flood of 17–18 January 1986. *Weather Forecast.* **1999**, *14*, 687–700. [CrossRef]

69. Ma, X.; Xie, F.; Li, J.; Zheng, X.; Tian, W.; Ding, R.; Sun, C.; Zhang, J. Effects of Arctic Stratospheric Ozone Changes on Spring Precipitation in the Northwestern United States. *Atmos. Chem. Phys.* **2019**, *19*, 861–875. [CrossRef]

70. Welker, J.M. Isotopic (δ18O) Characteristics of Weekly Precipitation Collected across the USA: An Initial Analysis with Application to Water Source Studies. *Hydrol. Processes* **2000**, *14*, 1449–1464. [CrossRef]

71. Li, S.; Levin, N.E.; Chesson, L.A. Continental Scale Variation in 17O-Excess of Meteoric Waters in the United States. *Geochim. Et Cosmochim. Acta* **2015**, *164*, 110–126. [CrossRef]

72. Kennedy, C.D.; Bowen, G.J.; Ehleringer, J.R. Temporal Variation of Oxygen Isotope Ratios (Δ18O) in Drinking Water: Implications for Specifying Location of Origin with Human Scalp Hair. *Forensic Sci. Int.* **2011**, *208*, 156–166. [CrossRef] [PubMed]

73. Bowen, G.J.; Cai, Z.; Fiorella, R.P.; Putman, A.L. Isotopes in the Water Cycle: Regional- to Global-Scale Patterns and Applications. *Annu. Rev. Earth Planet. Sci.* **2019**, *47*, 453–479. [CrossRef]

74. Froehlich, K.; Gibson, J.J.; Aggarwal, P.K. *Deuterium Excess in Precipitation and Its Climatological Significance*; International Atomic Energy Agency (IAEA): Vienna, Austria, 2002; pp. 54–66.

75. Bershaw, J.; Hansen, D.D.; Schauer, A.J. Deuterium Excess and 17O-Excess Variability in Meteoric Water across the Pacific Northwest, USA. *Tellus B Chem. Phys. Meteorol.* **2020**, *72*, 1–17. [CrossRef]

76. U.S., Department of Agriculture, U.S. Soil Conservation Service, West National Technical Center, Water Supply Forecasting Center, Snow Survey Sampling Guide, Agriculture Handbook 169, GPO 594-305, 1984. Available online: https://www.nrcs.usda.gov/wps/wcm/connect/wcc/89bb470a-b54c-4d22-a205-42e47c886293/SnowSurveySamplingGuideHandout.pdf?MOD=AJPERES&CVID=mnjJXyZ&CVID=mnjJXyZ (accessed on 19 April 2021).

77. Dansgaard, W. Stable Isotopes in Precipitation. *Tellus* **1964**, *16*, 436–468. [CrossRef]

78. Gat, J.R.; Carmi, I. Evolution of the Isotopic Composition of Atmospheric Waters in the Mediterranean Sea Area. *J. Geophys. Res.* **1970**, *75*, 3039–3048. [CrossRef]